Research Article

Received: 16 May 2011 Revised: 8 August 2011 Accepted: 3 September 2011 Published online in Wiley Online Library: 9 December 2011

(wileyonlinelibrary.com) DOI 10.1002/pi.3220

Strong resistance of poly (ethylene glycol) based L-tyrosine polyurethanes to protein adsorption and cell adhesion

Jui-Chen Yang,[a†] Chao Zhao,[a†] I-Fan Hsieh,[b] Senthilram Subramanian,[a] Lingyun Liu,[a] Gang Cheng,[a] Lingyan Li,[a] Stephen Z. D. Cheng[b] and Jie Zheng[a*]

Abstract

Biofouling that involves protein adsorption, cell and bacteria adhesion, and biofilm formation between a surface and biological entities is a great challenge for biomedical and industry applications. In this work, L-tyrosine-derived polyurethanes (L-polyurethane) with different molecular weights of poly(ethylene glycol) (PEG) were synthesized, characterized and coated on gold surfaces using spin-coating. The non-fouling activity of different L-polyurethane films was evaluated by protein adsorption and cell adhesion. Surface plasmon resonance and cell assay results demonstrate that the PEG content in these L-polyurethanes contributes excellent resistance to protein adsorption and cell attachments. This work provides alternative and effective biomaterials for potential applications in blood-contacting devices.

Keywords: antifouling; polyurethane; poly(ethylene glycol); surface resistance

INTRODUCTION

Development of biocompatible protein-resistant materials and surfaces is critical for many applications, such as biomedical diagnostics, tissue engineering, drug carriers, biosensors and marine coatings.[1,2] In particular, for materials in contact with blood, plasma and serum, even 5 ng cm^{-2} of fibrinogen adsorptions can induce full-scale blood platelet adhesion, causing implantable device failure and adverse outcomes for the patients.[3] There are two types of antifouling materials: some are hydrophilic-based materials, and the others are zwitterionic-based materials. Hydrophilic materials such as poly(ethylene glycol) (PEG),[4–7] hydroxy-functional methacrylates,[8,9] dextran,[10] mannitol[11] and glycerol dendron[12] mainly achieve surface hydration via hydrogen bonds, while zwitterionic-based materials such as phosphorylcholine-based materials,[13–15] sulfobetaine methacrylate[16] and carboxy-betaine methacrylate (CBMA)[17] achieve surface hydration via ionic induced hydration that can bind water molecules even more strongly. Surface hydration (i.e. water barrier theory) has been postulated to account for non-fouling ability,[18,19] in which tightly bound water layers adjacent to the surfaces can form a physical and energetic barrier to prevent proteins approaching the surface.

Among different classes of polymers used in the biomedical field, polyurethanes exhibit excellent biocompatibility and mechanical properties.[20–22] However, the thromboresistivity of polyurethanes still needs to be improved. We previously synthesized L-tyrosine-derived polyurethanes (L-polyurethanes) by using the condensation polymerization method to study their degradation, water absorption–release behavior, and mechanical properties *in vitro*.[23,24] Our L-tyrosine-based polyurethane consists of a hydrophilic soft segment of PEG units to enhance antifouling properties and a hydrophobic hard segment to improve mechanical properties. We have demonstrated that polyurethanes with modified L-tyrosine-derived pseudo-polyamide linkages in backbones greatly improved biocompatibility, biodegradability and nontoxicity for drug delivery.

Unlike conventional polyurethanes, which have been widely investigated for various biomedical applications, L-polyurethanes have so far not been tested for their non-fouling ability. In this work, we synthesize a series of L-polyurethanes consisting of a soft segment of PEG with different molecular weights (M_w 200, 600, 1000, 1500 and 4600), a linear diisocyanate hard segment of hexamethylene diisocyanate (HDI) and a diphenolic chain extender desaminotyrosine tyrosyl hexyl ester (DTH) by using two-step condensation polymerization. The biocompatibility and mechanical stability of L-polyurethanes are determined by both the soft segments of PEG units and the hard segments of diisocyanate and chain extender. The PEG is used to prevent nonspecific protein adsorption, the diisocyanate is used to enhance mechanical properties and the amino acid based chain extender DTH is used to maintain biocompatibility for different biomedical applications. We demonstrate that L-polyurethanes exhibit strong antifouling

* *Correspondence to: Jie Zheng, Department of Chemical and Biomolecular Engineering, University of Akron, Akron, OH 44325, USA. E-mail: zhengj@uakron.edu*

† *These authors contributed equally to this work.*

a *Department of Chemical and Biomolecular Engineering, University of Akron, Akron, OH 44325, USA*

b *Department of Polymer Science, University of Akron, Akron, OH 44325, USA*

resistance to both protein adsorption (fibrinogen, lysozyme and bovine serum albumin (BSA)) and cell adhesion.

MATERIALS AND METHODS

Materials

PEG (M_w = 200, 600, 1000, 1500 and 4600), L-tyrosine, thionyl chloride, desaminotyrosine, *N*-ethyl-*N*′-(3-dimethylaminopropyl) carbodiimide hydrochloride, HDI, 1-dodecanethiol, 11-mercapto-11-undecanol, tetrahydrofuran and phosphate buffered saline (0.01 mol L^{-1} PBS: NaCl 0.138 mol L^{-1} and KCl 0.0027 mol L^{-1}; pH 7.4) were purchased from Sigma-Aldrich (Milwaukee, WI, USA). *N*,*N*-dimethylformamide (DMF) was purchased from EMD Chemical Inc. *n*-Hexanol, ethyl ether, hexane and chloroform were obtained from Fisher Scientific. Fibrinogen (function I from bovine plasma), lysozyme (L6876) and BSA (BSA A7638) were purchased from Sigma-Aldrich. Ethanol (absolute 200 proof) was purchased from AAPER Alcohol and Chemical Co. PEG was dried in a vacuum oven at 40 °C for 24 h before use. DMF was dehydrated by calcium hydride and filtered prior to synthesis. Water used in these experiments was purified by a Millipore water purification system with a maximum resistivity of 18.0 MΩ cm.

Synthesis of L-polyurethanes

The synthesis of L-polyurethanes mainly involves two steps: (1) synthesis of the chain extender DTH by a carbodiimide-mediated condensation reaction as reported in our previous work[24] and (2) synthesis of the polyurethane by a condensation reaction. A two-step condensation polymerization[23] was performed to synthesize linear L-polyurethanes by introducing PEG with different molecular weights as the macrodiol, HDI as the diisocyanate and DTH as the chain extender (Scheme 1). Briefly, PEG polydiol was added to 40 mL dried DMF, followed by HDI addition. The mixture of PEG polydiol and HDI (1 : 2 molar) was stirred for 3 h at 85 °C to form PEG-prepolymer. Subsequently, the PEG-prepolymer was cooled to room temperature and DTH (1 : 1 molar ratio of PEG polydiol : DTH) was added to the solution and stirred for 12 h at 80 °C. To obtain the M_w of PEG below 1500, sodium chloride solution was used to precipitate polyurethane that was then washed with deionized water for several times to remove DMF; to obtain the L-polyurethane with the M_w of PEG above 4600, ethyl ether and hexane were used to precipitate polyurethane. The polyurethanes were dried in a vacuum oven under 40 °C for 48 h prior to any characterization and application. The detailed compositions of the polyurethanes are shown in Table 1.

Table 1. Composition of PEG-based L-tyrosine polyurethanes

Polyurethanes	Polydiol (M_w)	Soft segment (wt%)	Hard segment (wt%) Diisocyanate (HDI)	Hard segment (wt%) Chain extender (DTH)
$PEG_{(200)}$-HDI-DTH	PEG (200)	21.1	35.4	43.5
$PEG_{(600)}$-HDI-DTH	PEG (600)	44.4	25.0	30.6
$PEG_{(1000)}$-HDI-DTH	PEG (1000)	57.2	19.2	23.6
$PEG_{(1500)}$-HDI-DTH	PEG (1500)	66.8	15.0	18.2
$PEG_{(4600)}$-HDI-DTH	PEG (4600)	86.0	6.3	7.7

Characterization of L-polyurethane

The structure of L-polyurethanes was characterized by Fourier transform infrared (FTIR) spectroscopy and TGA. FTIR characterizations were performed with a Nexus 870-FTIR coupled with an attenuated total reflection (ATR) attachment and a germanium crystal. Spectra were collected at a resolution of 2 cm^{-1} with a sampling area of 3 mm^2. The decomposition temperature of L-polyurethanes was determined using a TA 2950 TGA. The operating temperature was increased from 25 °C to 600 °C at a rate of 20 °C min^{-1} under nitrogen. The decomposition temperature was taken to be when the L-polyurethane showed 5% weight loss.

Spin-coating of L-polyurethane on surface plasmon resonance (SPR) chips

A SPR glass chip (32 × 18 × 2 mm) was first coated with an adhesion-promotion chromium layer (thickness *ca* 2 nm) and a surface plasmon active gold layer (thickness *ca* 48 nm) by electron beam evaporation under vacuum. Before L-polyurethane coating, the SPR chip was washed with ethanol and deionized water, cleaned by UV ozone for 20 min, and washed with ethanol and deionized water again. The 0.5% (wt/wt) L-polyurethanes in chloroform solution were spin-coated on the SPR chips to form a thin film by an in-house spin-coating system P6700. The spin coater was set at 6000 rpm for 90 s under nitrogen, and samples were dried under vacuum at room temperature for 24 h prior to thickness measurements and SPR experiments.

Self-assembled monolayer (SAM) preparation on SPR chips

To prepare SAMs on the SPR chips, the cleaned gold-coated substrates were soaked in 0.1 mmol L^{-1} ethanol solution of

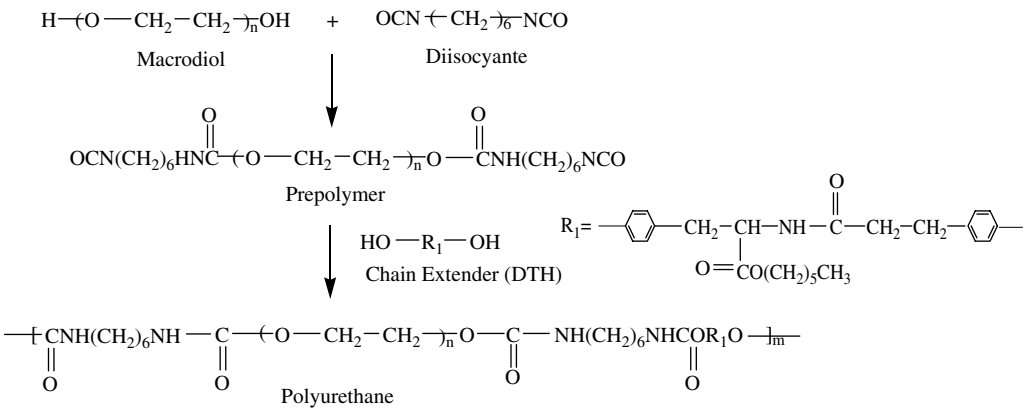

Scheme 1. Reaction steps for the synthesis of PEG-based L-tyrosine polyurethanes.

1-dodecanethiol or 11-mercapto-11-undecanol to form methyl-terminated SAMs (CH_3-SAMs) and hydroxyl-terminated SAMs (OH-SAMs), respectively. The substrates were washed sequentially with ethanol and deionized water and dried in a stream of clean compressed air before use.

Determination of film thickness by ellipsometry

The thickness of L-polyurethane film was measured with a Gaertner model L116C ellipsometer with He-Ne laser ($\lambda = 632.8$ nm). Six separate locations of each sample were measured at three different angles of incidence (40°, 60° and 80°) to obtain the average thickness of the polymer film. To achieve sensitive SPR signals, the film thickness was controlled at 26–31 nm by changing spin speed and solution concentration.

Contact angle measurements

Water contact angles of the L-polyurethane-coated surfaces and SAM surfaces were measured by the sessile drop technique on a Rame-Hart goniometer (Model 100-00, Mountain Lake, NJ, USA) using deionized water under ambient conditions. The averages of three readings from five different parts of the films were taken for each sample and reported as mean ± standard deviation.

Protein adsorption by SPR

Protein adsorption was measured by a custom-built four-channel SPR sensor, which is based on wavelength interrogation. The glass plate containing the spin-coated L-polyurethane was attached to the base of the prism, and an optical interface was established using a refractive index matching fluid (Cargille). A baseline signal was established by flowing PBS buffer at a rate of 50 µL min^{-1} through the sensor for 10 min. Freshly prepared protein solutions of fibrinogen, lysozyme and BSA in PBS (1 mg mL^{-1}) were administered into independent channels using a peristaltic pump (Ismatec) at 50 µL min^{-1} for 10 min, followed by PBS buffer solution to remove unbound proteins and to re-establish the baseline. Protein adsorption was quantified by the difference in wavelength between two buffer baselines established before and after protein adsorption. For the SPR sensor used in this work, a 1 nm wavelength shift at 750 nm represented 15 ng cm^{-2} of adsorbed protein. The amount of adsorbed proteins on the L-polyurethane films was compared with that of adsorbed proteins on the CH_3-SAM and OH-SAM. Since we used a four-channel SPR sensor, three channels were used to measure protein adsorption from the same protein solution and one channel was used for the control experiment. Thus, each SPR data point was repeated with three independent L-polyurethane-coated chips.

Cell adhesion

NIH/3T3 fibroblasts were cultured and grown in Dulbecco's modified Eagle's medium (DMEM), supplemented with 10% fetal bovine serum (FBS), 1% sodium pyruvate, 1% nonessential amino acids and 2% penicillin streptomycin solution at 37 °C in a humidified atmosphere containing 5% CO_2 on tissue culture polystyrene flasks. Fibroblasts were detached from flask surfaces by washing three times with 10 mL PBS, followed by incubation in 2 mL of trypsin/ethylenediaminetetraacetic acid (0.05/0.53 mmol L^{-1}). After cells were detached, they were resuspended in 8 mL of DMEM and the suspension was centrifuged at 1000 rpm for 5 min. The supernatant was removed, and the cells were diluted in DMEM with 0.2% FBS at a final concentration of 10^5 cells mL^{-1}. The L-polyurethane- or SAM-coated surfaces were placed in a 24-well plate and washed with PBS; 2 ml of cell suspension was then added to each well and incubated with the samples for 96 h. The morphology and proliferation of the cells were observed using an Olympus BX52 with Olympus DP70 CCD in reflection mode using a 5× objective.

RESULTS AND DISCUSSION

Characterization of L-polyurethane films

Five l-polyurethanes with different PEG units were synthesized and spin-coated on gold-coated substrates. This physisorption strategy is convenient for preparing antifouling surfaces without introducing a relatively complex chemisorption or covalent grafting for surface attachment. The prepared l-polyurethane surfaces were characterized using ATR-FTIR, ellipsometry and contact angle measurements. Figure 1 shows the FTIR spectra for five l-polyurethanes with different PEG molecular weights of 200, 600, 1000, 1500 and 4600. The spectra show a strong band at 1100 cm^{-1} representing the typical aliphatic ether functional group (C–O–C stretching) of PEG, a 1540 cm^{-1} band representing N–H bending/C–N stretching of urethane linkages and the amide linkage of the DTH segment, and a 1620 cm^{-1} band representing the aromatic stretch of the DTH segment. The characteristic peaks in the region 1715–1730 cm^{-1} represent the carbonyl of the urethane linkages. The distribution of the carbonyl peak indicates a degree of hydrogen bonding of the urethane carbonyl group and interactions between different segments. Moreover, a peak at 2900 cm^{-1} represents aliphatic CH_2 stretching, and the broad shoulder at 3330 cm^{-1} corresponds to N–H stretching, indicating the formation of urethane linkages. The decrease of the N–H signal as a function of the PEG molecular weight increase indicates the lesser amount of the urethane segment in the polymer. One of the two peaks from the C–H stretching signal increases, showing an increase of the PEG segment. The intensity of the other peak from the C–H stretching signal decreases, indicating the decrease

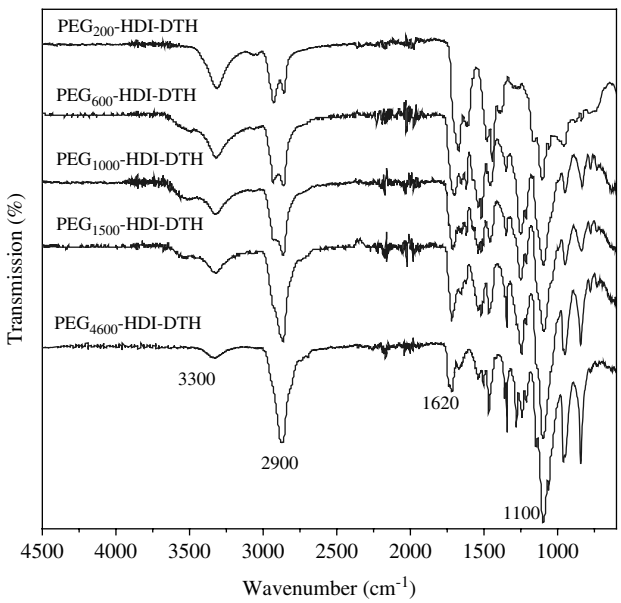

Figure 1. FTIR spectra of L-polyurethanes on a gold substrate with characteristic peaks: 1100 cm^{-1} O–C stretching; 1620 cm^{-1} C=C stretching; 2900 cm^{-1} C–H stretching; and 3330 cm^{-1} N–H stretching.

Table 2. Surface characterization of L-polyurethanes, OH-SAM and CH_3-SAM

Surface	Contact angle (°)	Thickness (nm)
$PEG_{(200)}$-HDI-DTH	79.0 ± 1.2	31.4 ± 4.5
$PEG_{(600)}$-HDI-DTH	65.2 ± 2.0	31.0 ± 2.0
$PEG_{(1000)}$-HDI-DTH	54.6 ± 4.9	27.1 ± 3.1
$PEG_{(1500)}$-HDI-DTH	37.1 ± 1.4	26.1 ± 2.3
$PEG_{(4600)}$-HDI-DTH	26.3 ± 3.6	26.3 ± 3.6
OH-SAM	5.8 ± 0.5	
CH_3-SAM	101.6 ± 1.6	

of the urethane segment. The FTIR data clearly demonstrate the existence of l-polyurethanes on the gold-coated glass.

The surface hydrophobicity of L-polyurethanes with different PEG_{200}, PEG_{600}, PEG_{1000}, PEG_{1500} and PEG_{4600} segments is characterized by static water contact angle measurements, in comparison with pure OH-SAM and CH_3-SAM. It can be seen from Table 2 that an increment in PEG molecular weight in the L-polyurethanes from 200 to 4600 greatly reduces contact angles from 79.0° to 29.3°, improving the hydrophilic nature of the polymer surfaces. The FTIR and contact angle results indicate that the L-polyurethanes with a low molecular weight of PEG units are relatively heterogeneous with mixed hard and soft segments, whereas increasing the molecular weight of PEG leads to increasing hydrogen binding of the urethane carbonyl within the hard segment domain and the formation of a cohesive and ordered hard segment. Hydrophobic and hard segments of HDI-DTH are physically adsorbed and embedded on the bare gold surface by strong hydrophobic interactions, while hydrophilic and flexible PEG segments are oriented towards the solvent. It was expected that the increased hydrophilicity, due to the increased PEG units, would improve surface hydration and non-fouling properties based on the water barrier theory.[18,19,25]

Our recent studies[8,9] have shown that poly(2-hydroxyethyl methacrylate) (polyHEMA) and poly(hydroxypropyl methacrylate) (polyHPMA) brushes at an appropriate film thickness of *ca* 20–45 nm show undetectable nonspecific protein adsorption (<0.3 ng cm^{-2}) from single-protein solutions. Thus, the thickness of different L-polyurethane films, as measured by ellipsometry, was controlled at *ca* 26–31 nm by tuning the spin-coating speed and solution concentration to achieve the best non-fouling performance and to acquire the sensitive SPR signals (Table 2). Additionally, the stability of polymer films in physiological conditions is very important for biomedical applications, because unstable polymer brushes can induce undesirable or unexpected loss of biological function and activity of biomaterials. The resistance to heat of the L-polyurethanes was examined by TGA (see Fig. 2 and Table 3). It can be seen that the decomposition temperatures of the L-polyurethanes increased from 251 °C to 314 °C as the PEG molecular weight increased from 200 to 4600, suggesting that all L-polyurethane polymers are thermally stable and can tolerate sterilization.

Protein adsorption on L-polyurethane surfaces

The adsorption of three proteins with different sizes and isoelectric points (pI), fibrinogen (Fib, pI = 5.5, 340 kD), BSA (pI = 4.9, 66 kD) and lysozyme (Lyz, pI = 11, 14 kD), on the L-polyurethane surfaces was quantified by an in-house

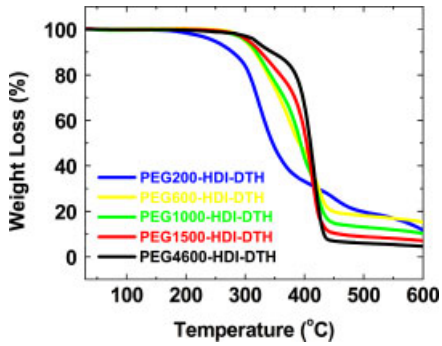

Figure 2. TGA analysis of the L-polyurethane.

Table 3. Decomposition temperature of L-polyurethanes

L-polyurethane	Decomposition temperature (°C)
$PEG_{(200)}$-HDI-DTH	*ca* 251
$PEG_{(600)}$-HDI-DTH	*ca* 300
$PEG_{(1000)}$-HDI-DTH	*ca* 301.8
$PEG_{(1500)}$-HDI-DTH	*ca* 304.5
$PEG_{(4600)}$-HDI-DTH	*ca* 314.3

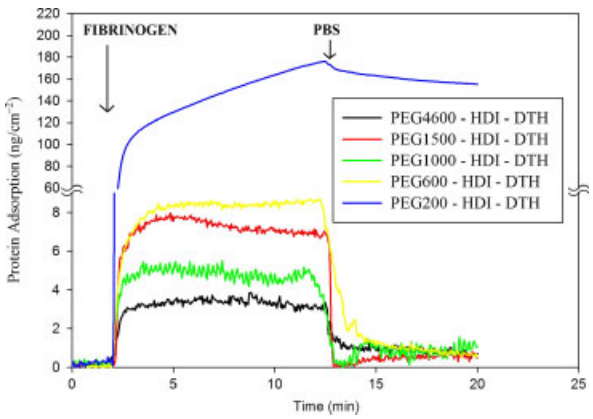

Figure 3. Typical SPR sensorgrams of fibrinogen adsorption on five L-polyurethanes, OH-SAM and CH_3-SAM.

four-channel SPR sensor, in comparison with OH-SAM and CH_3-SAM surfaces. Figure 3 shows a typical SPR sensorgram of Fib on different surfaces. It can be seen that, except for the PEG_{200}-L-polyurethane, all other L-polyurethane films showed almost undetectable nonspecific Fib adsorption (<0.3 ng cm^{-2}), compared with significant Fib adsorption of 345 ng cm^{-2} on hydrophobic CH_3-SAM and 150 ng cm^{-2} on hydrophilic OH-SAM, consistent with previous experiments.[15] Similar trends were observed for BSA and Lyz adsorption on the L-polyurethane surfaces. Specifically, L-polyurethane films with PEG_{1000}, PEG_{1500} and PEG_{4600} can achieve a super-low fouling level (protein adsorption < 5 ng cm^{-2}), as shown in Fig. 4, similar to the level of adsorbed proteins on OEG-SAM,[27] polyCBMA,[17] polyHEAA[26] and polyHPMA.[8] A large amount of proteins adsorbed on the PEG_{200}-L-polyurethane could be attributed to the fact that shorter PEG chains cannot cover the whole surface, leading to more hydrophobic HDI-DTH segments exposed to protein solution, as evidenced by the large contact angle of *ca* 79° (Table 2).

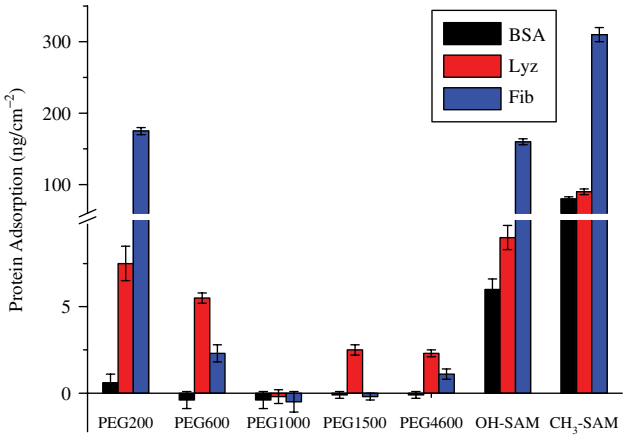

Figure 4. Adsorption of 1 mg mL^{-1} fibrinogen (Fib), lysozyme (Lyz) and BSA on L-polyurethanes with different molecular weights of PEG, OH-SAM and CH_3-SAM surfaces as measured by SPR.

The non-fouling property of a given surface is often theoretically explained by the formation of a hydration layer near the surface[28,29] because a tightly bound water layer forms a physical and energetic barrier to prevent proteins being adsorbed on the surface. The strength of the hydration layer is primarily determined by the physicochemical properties of the surface (i.e. surface chemistry, surface packing density and film thickness). But it is a very challenging task to directly measure the associated water molecules on the surface by experiments. It can be seen that, although the OH-SAM surface has a much smaller contact angle than the polyurethane, SPR data show that the L-polyurethane surfaces with large PEG molecular weights exhibit an excellent resistance to protein adsorption compared with the OH-SAM. This is because the polymer films (>26 nm in thickness) are significantly thicker than the SAM (*ca* 3–5 nm in thickness),[30] and as a result more 'non-fouling' ethylene oxide units at the interface will interact with water to create a stronger hydration layer to resist protein adsorption. Apart from the increased non-fouling interactions, polymer film is very flexible, so when protein approaches the surface the compression of the polymer chains leads to an unfavorable decrease in entropy (i.e. repulsive force) to resist protein adsorption.

Long-term cell adhesion on L-polyurethane surfaces

A polymer surface that effectively resists protein adsorption does not necessarily resist cell adhesion and even biofilm formation,[19] because cells can adapt themselves to survive in a very harsh environment by initially attaching to and then proliferating on surfaces. *In situ* long-term cell adhesion was also studied. Figure 5 shows optical images of different surfaces in contact with NIH/3T3 fibroblasts at a magnification of 5×. The bare gold surface was largely covered by NIH/3T3 fibroblasts after culturing NIH/3T3 cells at 37 °C for 3 days (Figs 5(c), 5(d)), while the PEG_{1000}-L-polyurethane surface was barely covered by a few cells after 4 days (Figs 5(a), 5(b)).

CONCLUSIONS

In this work, a series of L-polyurethanes with different molecular weights of PEG were synthesized, characterized and spin-coated on gold substrates. SPR results demonstrate that L-polyurethane films with PEG_{1000}, PEG_{1500} and PEG_{4600} with a relatively high PEG molecular percentage of 57.2%, 66.8% and 86.0%, respectively, can achieve a comparable protein adsorption of <5 ng cm^{-2} at a super-low fouling level. Cell assay results also show that L-polyurethane surfaces can greatly inhibit NIH/3T3 attachments within 4 days. This work provides new and efficient ultra-low fouling polymer surfaces for biomedical applications.

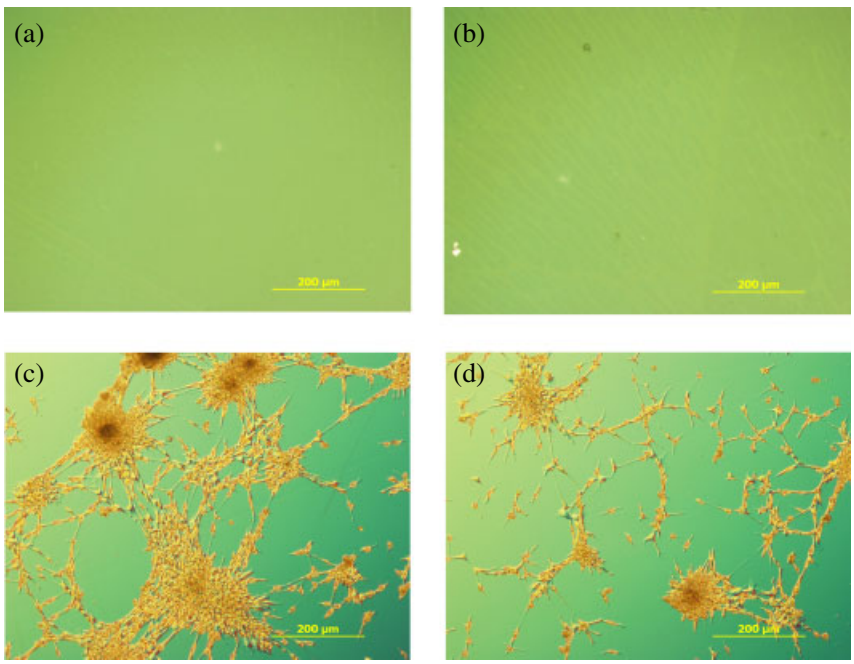

Figure 5. Representative microscopic images of NIH/3T3 fibroblast adhesion on (a), (b) the L-polyurethane with PEG_{1000} after 96 h and (c), (d) the bare gold surface after 72 h.

ACKNOWLEDGEMENT

J.Z. is grateful for financial support from an NSF Career Award (CBET-0952624) and a 3M Non-Tenured Faculty Award. L.L. is grateful for financial support from Cleveland Clinic Foundation/Clinical Tissue Engineering Center (TECH-09-006A) and Firestone Research Initiative Fellowship.

REFERENCES

1 Morra M, *J Biomater Sci Polym Ed* **11**:547–569 (2000).
2 Ratner BD and Bryant SJ, *Ann Rev Biomed Eng* **6**:41–75 (2004).
3 Shen MC, Wagner MS, Castner DG, Ratner BD and Horbett TA, *Langmuir* **19**:1692–1699 (2003).
4 Zoulalian V, Zürcher S, Tosatti S, Textor M, Monge S and Robin J-J, *Langmuir* **26**:74–82 (2009).
5 Kingshott P, Wei J, Bagge-Ravn D, Gadegaard N and Gram L, *Langmuir* **19**:6912–6921 (2003).
6 Harbers GM, Emoto K, Greef C, Metzger SW, Woodward HN, Mascali JJ, *et al*, *Chem Mater* **19**:4405–4414 (2007).
7 Chang Y, Chu W-L, Chen W-Y, Zheng J, Liu L, Ruaan R-C, *et al*, *J Biomed Mater Res A* **93A**:400–408 (2010).
8 Zhao C, Li L and Zheng J, *Langmuir* **26**:17375–17382 (2010).
9 Zhao C, Li L, Wang Q, Yu Q and Zheng J, *Langmuir* **27**:4906–4913 (2011).
10 Martwiset S, Koh AE and Chen W, *Langmuir* **22**:8192–8196 (2006).
11 Luk YY, Kato M and Mrksich M, *Langmuir* **16**:9604–9608 (2000).
12 Wyszogrodzka M and Haag R, *Biomacromolecules* **10**:1043–1054 (2009).
13 Ishihara K, Nomura H, Mihara T, Kurita K, Iwasaki Y and Nakabayashi N, *J Biomed Mater Res A* **39**:323–330 (1998).
14 Nakabayashi N and Williams DF, *Biomaterials* **24**:2431–2435 (2003).
15 Chen S, Zheng J, Li L and Jiang S, *J Am Chem Soc* **127**:14473–14478 (2005).
16 Zhang Z, Chen S, Chang Y and Jiang S, *J Phys Chem B* **110**:10799–10804 (2006).
17 Zhang Z, Chen S and Jiang S, *Biomacromolecules* **7**:3311–3315 (2006).
18 Chen S, Li L, Zhao C and Zheng J, *Polymer* **51**:5283–5293 (2010).
19 Jiang S and Cao Z, *Adv Mater* **22**:920–932 (2010).
20 Zdrahala RJ and Zdrahala IJ, *J Biomaterials Appl* **14**:67–90 (1999).
21 Johnson PA, Luk A, Demtchouk A, Patel H, Sung H-J, Treiser MD, *et al*, *J Biomed Mater Res A* **93A**:505–514 (2010).
22 Guelcher SA, *Tissue Eng B – Rev* **14**:3–17 (2008).
23 Sarkar D, Yang J-C, Gupta AS and Lopina ST, *J Biomed Mater Res A* **90A**:263–271 (2009).
24 Gupta AS and Lopina ST, *J Biomater Sci Polym Ed* **13**:1093–1104 (2002).
25 Zheng J, He Y, Chen S, Li L, Bernards MT and Jiang S, *J Chem Phys* **125**:174714–174717 (2006).
26 Zhao C and Zheng J, *Biomacromolecules*, **12**:4071–4079 (2011).
27 Li L, Chen S, Zheng J, Ratner BD and Jiang S, *J Phys Chem B* **109**:2934–2941 (2005).
28 Zheng J, Li L, Tsao H-K, Sheng Y-J, Chen S and Jiang S, *Biophys J* **89**:158–166 (2005).
29 Herrwerth S, Eck W, Reinhardt S and Grunze M, *J Am Chem Soc* **125**:9359–9366 (2003).
30 Ladd J, Zhang Z, Chen S, Hower JC and Jiang S, *Biomacromolecules* **9**:1357–1361 (2008).

